Tunable focal shift induced by polarization and phase shaping

Zhang, Shuoshuo; Bai, Zhidong; Li, Jinjian; Lyu, Yudong; Man, Zhongsheng; Xing, Fei; Ge, Xiaolu; Fu, Shenggui

DOI
10.1016/j.ijleo.2019.04.134

Publication date
2019

Document Version
Final published version

Published in
Optik

Citation (APA)
Zhang, S., Bai, Z., Li, J., Lyu, Y., Man, Z., Xing, F., Ge, X., & Fu, S. (2019). Tunable focal shift induced by polarization and phase shaping. *Optik*, *199*, Article 162788. https://doi.org/10.1016/j.ijleo.2019.04.134

Optik - International Journal for Light and Electron Optics 199 (2019) 162788

Contents lists available at ScienceDirect

Optik

journal homepage: www.elsevier.com/locate/ijleo

Original research article

Tunable focal shift induced by polarization and phase shaping

Shuoshuo Zhang[a], Zhidong Bai[a], Jinjian Li[a], Yudong Lyu[a], Zhongsheng Man[a,b], Fei Xing[a], Xiaolu Ge[a], Shenggui Fu[a,*]

[a] School of Physics and Optoelectronic Engineering, Shandong University of Technology, Zibo, 255000, China
[b] Optics Research Group, Delft University of Technology, Department of Imaging Physics, Lorentzweg 1, 2628CJ, Delft, the Netherland

ARTICLE INFO

Keywords:
Focal shift
Singular optics
Diffractive optics
Polarization

ABSTRACT

We propose a simple method to control the move and elongation of focus along the optical axis in a high-numerical aperture focusing system. By introducing the optical degree of freedom of polarization in the radial direction, a tunable focal shift and elongation of focus are achieved simply by tailoring the polarization index and the topological charge of vortex phase, without the need of additional modulations of amplitude or diffractive optical elements. These findings may be of help in the applications like optical micro-manipulation, laser processing, and imaging.

1. Introduction

Focal shift, which is referred to the physical phenomenon that the point of maximum intensity of focused electric field does not coincide with the geometric focus but is shifted to somewhere along optical axis [1], has attracted considerable attention due to its practical and potential applications like optical imaging [2], optical alignment [3], and optical coherence tomography systems [4]. In the past few decades, such phenomenon has been investigated in various beams including Laguerre-Gaussian beams [5–8], Bessel-Gaussian beams [9,10], and flat-topped Gaussian beams [11,12]. And the initial studies mainly focus on the lights with homogenous states of polarization (SoPs), or neglect the polarization properties with scalar diffraction theory. In such a case, the magnitude of focal shift depends strongly on the Fresnel number or the effective Fresnel number of optical systems, and the focal shift occurs only under the conditions that the value of Fresnel number or effective Fresnel number is sufficiently small [13–17]. Additionally, some specially designed modulation devices are also adopted to achieve such a phenomenon, for example, tunable pupil filter [18,19], polarization mask [20,21], and Fresnel zone plate [22]. In general, all the aforementioned methods require a complicated adjustment process, which makes it difficult to shift the focus in real time.

Although the phenomenon of focal shift has been proposed and investigated in many systems, very few works are involved in the vector optical fields, which has a spatially-variant SoP in the beam cross-section compared with the scalar beams [23,24]. The focal shift in vector Bessel-Gaussian beams is firstly reported by Greene and Hall [25]. Thereafter, many groups have shown great interest in this realm and quantities of new phenomena have been found. For instance, Yan et al. have achieved the focal shift in a 4pi tightly focused system illuminated by two counter-propagating radially polarized beams [26,27]. The highlight of this work is to produce an almost spherical shaped spot in the focal region, which keeps unchanged during the whole shifting. However, this result relies on the precise control of a phase modulation function which may limit the practical applications. Yang et al. propose a new method to achieve the focal shift utilizing the spatially-variant polarized beams controlled by a liquid crystal variable retarder [28]. According to their simulations, the shift highly depends on the local polarization and system parameters. Specifically, it is larger for a narrower beam and longer wavelength. However, such shift can only appear in a limited range and the focus can only be moved towards the

* Corresponding author.
E-mail address: fushenggui@sdut.edu.cn (S. Fu).

https://doi.org/10.1016/j.ijleo.2019.04.134
Received 28 February 2019; Accepted 29 April 2019

negative direction of the optical axis, which restricts its further applications.

In this paper, we propose a simple and flexible method to achieve a tunable focal shift in a high numerical-aperture (NA) focusing system. We introduce the optical degree of freedom of polarization in the radial direction and propose a new light mode that possesses radially- and azimuthally-variant SoPs and vortex phase to modulate the focal field. Based on the Richards-Wolf vectorial diffraction theory [29], an analytical model which can be applied to calculate the three-dimensional focal electric field distributions of the proposed light is presented. Then, the focusing behaviors of radially- and azimuthally-variant vector vortex beams are systematically investigated and analyzed in detail. By calculations, it is found that a continuous shifting of focus in the both directions of optical axis can be achieved simply by tailoring the polarization index and the topological charge. These findings may be of help in the applications like optical micro-manipulation, laser processing, and imaging.

2. Theoretical model

Amplitude, polarization, and phase are three important parameters of a light beam. Mathematically, when referring to the famous cylindrical vector vortex beam, it can be described as follows [30]

$$\mathbf{E} = A\exp(im\varphi)[\cos(n\varphi)\hat{\mathbf{e}}_x + \sin(n\varphi)\hat{\mathbf{e}}_y], \tag{1}$$

where A represents the relative amplitude distribution, m is the topological charge of vortex phase, n is the polarization index determining the specific polarization distributions, φ is the azimuthal angle in the polar coordinate system. Obviously, the local SoP described by Eq. (1) only depends on the variable φ, thus they are azimuthally-variant polarized beams. If the optical degree of freedom of polarization in the radial direction is introduced, then the resultant beam can be given by

$$\mathbf{E} = A\exp(im\varphi)\left\{\cos\left[n\left(\varphi + 2\pi\frac{r}{r_0}\right)\right]\hat{\mathbf{e}}_x + \sin\left[n\left(\varphi + 2\pi\frac{r}{r_0}\right)\right]\hat{\mathbf{e}}_y\right\}, \tag{2}$$

Here, r and r_0 denote, respectively, the polar radius and the radius of input optical field. From Eq. (2), we can see that the local SoP depends on both the azimuthal angle φ and polar radius r now, hence it is a radially- and azimuthally-variant vector vortex beam. This type of vector beams can be generated in experiment with a spatial light modulator (SLM) and a common path interferometric arrangement [31–33].

Tightly focused optical fields are excellent tools for detailed studies in nano-optics including advanced fluorescence microscopy [34,35], optical trapping and manipulation [36,37], super resolution imaging [38–40], and nanoplasmonics [41–43]. Such optical fields can be obtained, for example, by focusing of input field through a high-NA objective lens, as depicted in Fig. 1. When the incident optical field is embodied by Eq. (2), the electric field in the vicinity of focus should be analyzed using the Richards-Wolf vectorial diffraction theory [33], because the contribution of input polarization cannot be neglected. According to the vectorial Richards-Wolf diffraction integration, we first derive the electric field expression of a tightly focused radially- and azimuthally-variant vector vortex beam in the cylindrical coordinate system (ρ, ϕ, z) as follows [29,44]

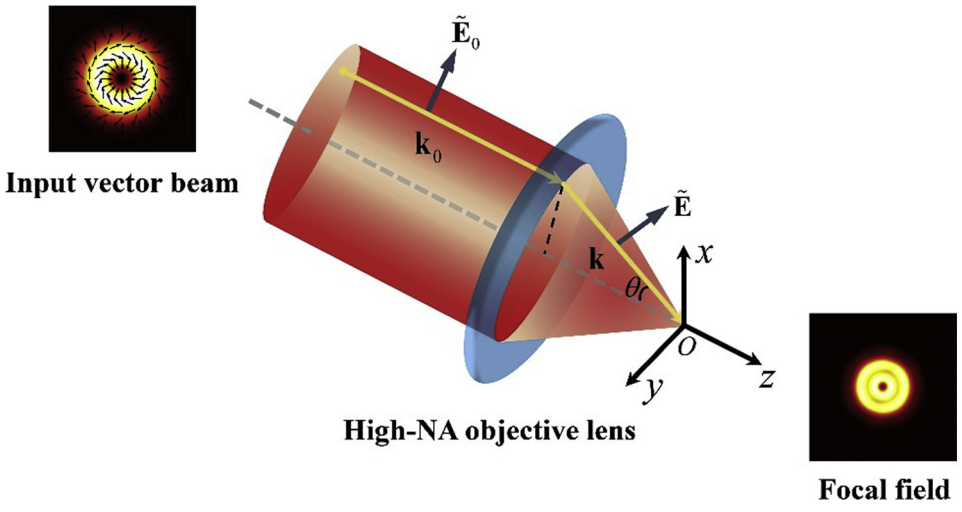

Fig. 1. Schematic diagram of the structure of a high-NA focusing system. The origin O of the Cartesian coordinate system coincide with the geometric focus.

$$E_x(\rho,\phi,z) = -\frac{ikf}{2\pi}\int_0^{2\pi}\int_0^{\alpha} l(\theta)\exp(im\varphi)\cos^{1/2}\theta\sin\theta \times\{\cos[(n-1)\varphi+2n\pi\frac{\sin\theta}{\sin\alpha}]\cos\theta\cos\varphi-\sin[(n-1)\varphi+2n\pi\frac{\sin\theta}{\sin\alpha}]\sin\varphi\} \times\exp\{ik[-\rho\sin\theta\cos(\varphi-\phi)+z\cos\theta]\}d\theta d\varphi, \tag{3a}$$

$$E_y(\rho,\phi,z) = -\frac{ikf}{2\pi}\int_0^{2\pi}\int_0^{\alpha} l(\theta)\exp(im\varphi)\cos^{1/2}\theta\sin\theta \times\{\cos[(n-1)\varphi+2n\pi\frac{\sin\theta}{\sin\alpha}]\cos\theta\sin\varphi+\sin[(n-1)\varphi+2n\pi\frac{\sin\theta}{\sin\alpha}]\cos\varphi\} \times\exp\{ik[-\rho\sin\theta\cos(\varphi-\phi)+z\cos\theta]\}\mathrm{d}\theta\mathrm{d}\varphi, \tag{3b}$$

$$E_z(\rho,\phi,z) = -\frac{ikf}{2\pi}\int_0^{2\pi}\int_0^{\alpha} l(\theta)\exp(im\varphi)\cos^{1/2}\theta\sin^2\theta \times\cos[(n-1)\varphi+2n\pi\frac{\sin\theta}{\sin\alpha}]\exp\{ik[-\rho\sin\theta\cos(\varphi-\phi)+z\cos\theta]\}\mathrm{d}\theta\mathrm{d}\varphi, \tag{3c}$$

Here, f is the focal length of high-NA objective lens; α is the maximum convergence angle that can be calculated by $\alpha=\arcsin(\mathrm{NA}/n_0)$, where NA is the numerical aperture of aplanatic objective lens, n_0 is the refractive index in image space; $l(\theta)$ is the pupil function which describes the relative amplitude distribution of incident field. Using the following transformations

$$E_\rho = E_x\cos\phi + E_y\sin\phi, \tag{4a}$$

$$E_\phi = E_y\cos\phi - E_x\sin\phi, \tag{4b}$$

We can also derive the radial and azimuthal components of electric field near the focus as

$$E_\rho(\rho,\phi,z) = -\frac{ikf}{2\pi}\int_0^{2\pi}\int_0^{\alpha} l(\theta)\exp(im\varphi)\cos^{1/2}\theta\sin\theta \times\{\cos[(n-1)\varphi+2n\pi\frac{\sin\theta}{\sin\alpha}]\cos(\varphi-\phi)\cos\theta-\sin[(n-1)\varphi+2n\pi\frac{\sin\theta}{\sin\alpha}]\sin(\varphi-\phi)\} \times\exp\{ik[-\rho\sin\theta\cos(\varphi-\phi)+z\cos\theta]\}\mathrm{d}\theta\mathrm{d}\varphi, \tag{5a}$$

$$E_\phi(\rho,\phi,z) = -\frac{ikf}{2\pi}\int_0^{2\pi}\int_0^{\alpha} l(\theta)\exp(im\varphi)\cos^{1/2}\theta\sin\theta \times\{\cos[(n-1)\varphi+2n\pi\frac{\sin\theta}{\sin\alpha}]\sin(\varphi-\phi)\cos\theta+\sin[(n-1)\varphi+2n\pi\frac{\sin\theta}{\sin\alpha}]\cos(\varphi-\phi)\} \times\exp\{ik[-\rho\sin\theta\cos(\varphi-\phi)+z\cos\theta]\}\mathrm{d}\theta\mathrm{d}\varphi, \tag{5b}$$

3. Calculations and analyses

Using Eqs. (2)–(5b), we can now explore the focal behaviors of radially- and azimuthally- variant vector vortex beams. In all our calculations, a Bessel-Gaussian beam is considered throughout this paper, which can be given as [44]

$$l(\theta)=\exp\left[-\beta^2\left(\frac{\sin\theta}{\sin\alpha}\right)^2\right]J_1\left(2\beta\frac{\sin\theta}{\sin\alpha}\right), \tag{6}$$

where β is defined as the ratio of the pupil radius and the beam waist, which we take as 1.5 in our configuration. $J_1(x)$ is the first-order Bessel function of the first kind. The NA of focusing lens is assumed to be 0.95, and the refractive index n_0 in image space is chosen as 1. Furthermore, all length measurements are in units of wavelengths.

By large calculations, we find that a tunable focal shift along the optical axis can occur only under the conditions that the absolute values between the topological charge m and the polarization index n are equal ($|m| = |n|$). Now we examine the situations when m and n are equal ($m = n$), as depicted Fig. 2, which shows the total electric field intensity distributions in the through-focus plane of six kinds of radially- and azimuthally-variant vector vortex beams with $m = n = -1, -2, -3, 1, 2$, and 3, respectively. All the images are normalized to their maximum intensities for each input light mode. Obviously, there exhibits a deviation between the point of maximum intensity and the geometric focus along the optical axis for all the input beam modes. Furthermore, the magnitude and direction of such deviation are controllable, depending on the value of m (or n). To be specific, the deviation will increase when $|m|$ (or $|n|$) grows, and it will shift along the $+(-)$ z direction when m (or n) is negative (positive). Moreover, the increase of deviation is always accompanying with the elongation of the depth of focus. These peculiar properties are very important in practical applications, because one can change the location of focus only by tailoring the intrinsic optical degrees of freedom including polarization and phase, without the need of adjusting the optical setup.

Next, we explore the conditions when m and n have opposite values ($m = -n$). As examples, we simulate the total electric field intensity distributions in the through-focus plane of six types of radially- and azimuthally-variant vector vortex beams with $(m, n) = (1, -1), (2, -2), (3, -3), (-1, 1), (-2, 2)$, and $(-3, 3)$, respectively, as depicted in Fig. 3, wherein all the images are normalized to

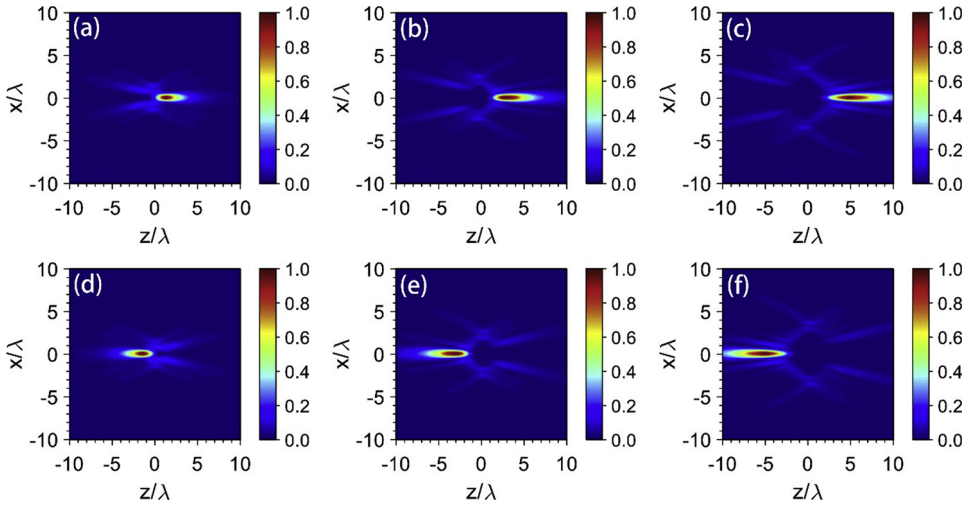

Fig. 2. Calculated total electric field intensity distributions in the through-focus plane of tightly focused radially- and azimuthally-variant vector vortex beams with $m = n =$ (a) -1, (b) -2, (c) -3, (d) 1, (e) 2, and (f) 3, respectively. All the images are normalized to their maximum intensities for each input light mode.

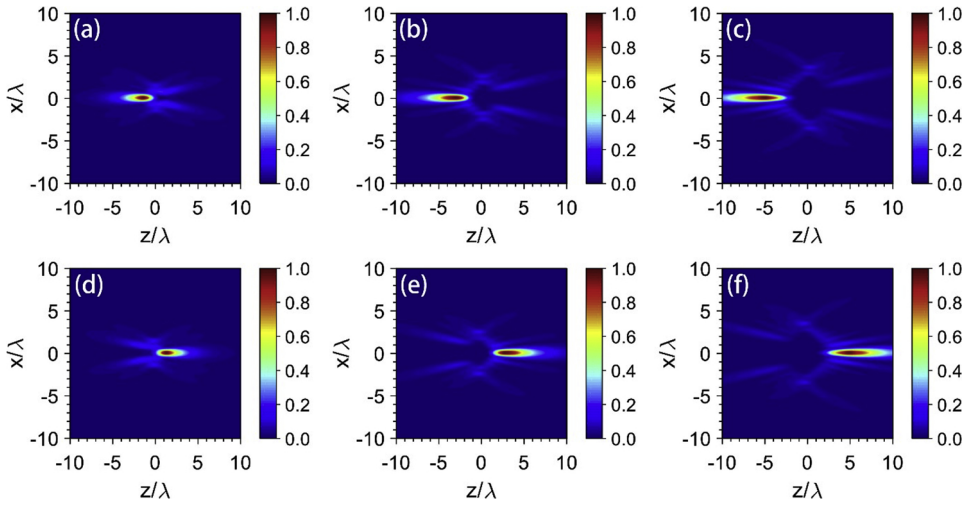

Fig. 3. Calculated total electric field intensity distributions in the through-focus plane of tightly focused radially- and azimuthally-variant vector vortex beams with $(m, n) =$ (a) $(1, -1)$, (b) $(2, -2)$, (c) $(3, -3)$, (d) $(-1, 1)$, (e) $(-2, 2)$, and (f) $(-3, 3)$, respectively. All the images are normalized to their maximum intensities for each input light mode.

the maximum intensity for each input light mode. That the phenomenon of focal shift is also apparent, similar as that in Fig. 2. By the comparisons between Figs. 2 and 3, we can easily find that the direction of focal shift only depends on the sign of topological charge m. Specifically, the focus will be shifted in the negative direction of z axis when m is positive, as depicted in Figs. 2(d)–(f) and 3 (a)–(c). Of course, the corresponding direction of focal shift will be reversed when m has a negative value, as shown in Figs. 2(a)–(c) and 3 (d)–(f).

To provide a better understanding of the focal shift and the elongation of the depth of focus, Fig. 4(a) gives the normalized focal field intensity profiles along the optical axis of all the aforementioned light modes depicted in Figs. 2 and 3. For the sake of comparison, the case of linearly polarized plane beam ($m = n = 0$) is also given under the same focusing conditions. For $m = n = 0$, the peak is located exactly at the geometric focus ($z = 0$), indicating that there is no focal shift. However, for other values of m and n, the phenomena of focal shift and elongation of the depth of focus happen. Specifically, the peak move forward and backward along the optical axis for a negative and positive value of m, respectively. And the magnitude of focal shift becomes more and more remarkable with the increases of $|m|$ and $|n|$. Further, we can see the peaks when m takes two opposite values are symmetric about the origin. As proved in Fig. 4(a), such focal shift and elongation of the depth of focus highly depend on the values of m and n, and they must satisfy $|m| = |n|$. For giving a detailed and quantitative studies of the influence induced by the input polarization and phase, Fig. 4(b) and (c) shows, respectively, the magnitude of focal shift and the depth of focus versus the topological charge m. Here, the magnitude of focal shift is defined as the distance between the peak and the origin, which is 13.025λ, 12.051λ, 9.622λ, 8.519λ, 6.312λ, 4.991λ,

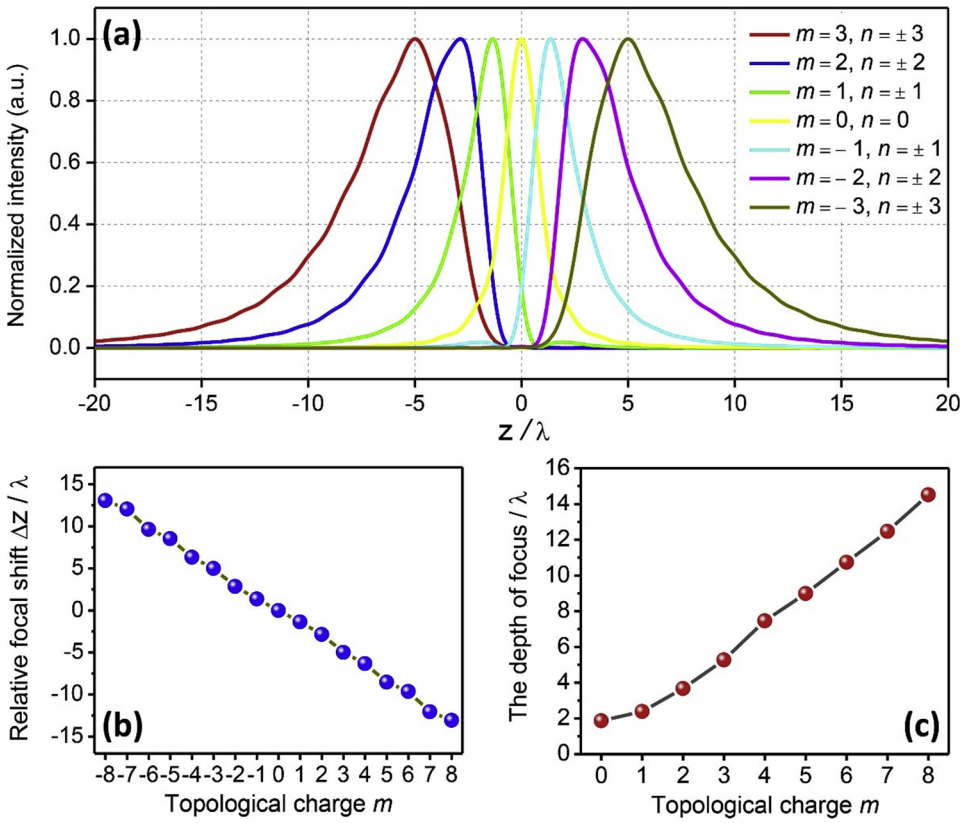

Fig. 4. (a) Normalized focal field intensity profiles along the optical axis for all the input beam modes depicted in Figs. 2 and 3. For comparison, the case of linearly polarized plane beam ($m = n = 0$) is also given under the same focusing conditions. (b) The magnitude of focal shift and (c) the depth of focus versus the topological charge m.

2.860λ, 1.356λ, 0, −1.356λ, −2.860λ, −4.991λ, −6.312λ, −8.519λ, −9.622λ, −12.051λ, and −13.052λ for the input modes with $m = -8, -7, -6, -5, -4, -3, -2, -1, 0, 1, 2, 3, 4, 5, 6, 7$, and 8, respectively. Since the depth of focus has many definitions, we use the full width at half maximum (FWHM) of the normalized electric field intensity profiles along the optical axis to evaluate the depth of focus in this paper. And the values are calculated to be about 1.868λ, 2.390λ, 3.674λ, 5.277λ, 7.455λ, 8.985λ, 10.734λ, 12.468λ, and 14.516λ for the input modes with $m = 0, 1, 2, 3, 4, 5, 6, 7$, and 8, separately.

4. Conclusion

To summarize, we have proposed a simple and flexible method to control the focal shift in a high-NA focusing system. We introduce the optical degree of freedom of polarization in the radial direction and propose a new kind of light mode that possesses radially- and azimuthally-variant SoPs and vortex phase. Based on the Richards-Wolf vectorial diffraction theory, an analytical model to calculate the three-dimensional electric field distributions near focus of the proposed radially- and azimuthally-variant vector vortex beams is presented. Based on such model, it is found that a continuous shifting of focus in the both directions of optical axis can be achieved simply by tailoring the polarization index and the topological charge of vortex phase. Further, the focal shift is always accompanying with the elongation of the depth of focus. These findings may be of help in the applications like optical micro-manipulation, laser processing, and imaging.

Acknowledgments

This work was partially supported by the National Natural Science Foundation of China (NSFC) (11604182); Natural Science Foundation of Shandong Province (ZR2016AB05).

References

[1] Y. Li, E. Wolf, Focal shifts in diffracted converging spherical waves, Opt. Commun. 39 (1981) 211–215.
[2] M. Yun, W. Liang, W. Kong, X. Gao, H. Zhu, J. Liang, Transverse superresolution and focal shift with rotational tunable phase mask, Opt. Commun. 283 (2010) 2079–2083.

[3] N. Manivannan, M.A.A. Neil, W. Balachandran, Optical alignment of pixelated 4f optical system using multiplexed filter, Appl. Opt. 52 (2013) 7812–7820.
[4] M. Pircher, E. Götzinger, C.K. Hitzenberger, Dynamic focus in optical coherence tomography for retinal imaging, J. Biomed. Opt. 11 (2006) 054013.
[5] W.H. Carter, M.F. Aburdene, Focal shift in Laguerre-Gaussian beams, J. Opt. Soc. Am. A 4 (1987) 1949–1952.
[6] Z. Ren, S. Qian, C. Tu, Y. Li, H. Wang, Focal shift in tightly focused Laguerre-Gaussian beams, Opt. Commun. 334 (2015) 156–159.
[7] M. Zhang, Y. Chen, L. Liu, Y. Cai, Focal shift of a focused partially coherent Laguerre-Gaussian beam of all orders, J. Mod. Opt. 63 (2016) 2226–2234.
[8] Y. Chen, S. Huang, M. Chen, X. Liu, Focal shift in tightly focused hybridly polarized Laguerre-Gaussian vector beams with zero radial index, J. Opt. Soc. Am. A 35 (2018) 1585–1591.
[9] B. Lü, W. Huang, Focal shift in unapertured Bessel-Gauss beams, Opt. Commun. 109 (1994) 43–46.
[10] B. Lü, W. Huang, Three-dimensional intensity distribution of focused Bessel-Gauss beams, J. Mod. Opt. 43 (1996) 509–515.
[11] R. Borghi, M. Santarsiero, S. Vicalvi, Focal shift of focused flat-topped beams, Opt. Commun. 154 (1998) 243–248.
[12] B. Ghafary, M. Alavinejad, H. Siampoor, Focal shift and focal switch of partially coherent flat-topped beams passing through an alignment and misalignment lens system with aperture, J. Mod. Opt. 57 (2010) 2075–2081.
[13] Y. Li, Dependence of the focal shift on Fresnel number and f number, J. Opt. Soc. Am. A 72 (1982) 770–775.
[14] W.H. Carter, Focal shift and concept of effective Fresnel number for a Gaussian laser beam, Appl. Opt. 21 (1982) 1989–1994.
[15] Y. Li, E. Wolf, Three-dimensional intensity distribution near the focus in systems of different Fresnel numbers, J. Opt. Soc. Am. A 1 (1984) 801–808.
[16] Y. Li, Focal shift in small-Fresnel-number focusing systems of different relative aperture, J. Opt. Soc. Am. A 20 (2003) 234–239.
[17] M. Dong, J. Pu, Effective Fresnel number and the focal shifts of focused partially coherent beams, J. Opt. Soc. Am. A 24 (2007) 192–196.
[18] M. Yun, E.H. Lee, Focal shift and extended focal depth with tunable pupil filter, J. Mod. Opt. 55 (2008) 2857–2863.
[19] P. Gao, S. Tian, X. Weng, H. Guo, Dynamically shifting the focal spot with tunable pupil filters, J. Mod. Opt. 63 (2016) 1558–1563.
[20] D.R. Chowdhury, K. Bhattacharya, A.K. Chakroborty, Focal shift in an imaging system with polarization-phase modulated aperture plane, J. Opt. 31 (2002) 117–128.
[21] D.R. Chowdhury, K. Bhattacharya, A.K. Chakroborty, R. Ghosh, Possibility of an optical focal shift with polarization masks, Appl. Opt. 42 (2003) 3819–3826.
[22] X. Liu, J. Pu, Focal shift and focal switch of partially coherent light in dual-focus systems, Opt. Commun. 252 (2005) 262–267.
[23] Q. Zhan, J.R. Leger, Focus shaping using cylindrical vector beams, Opt. Express 10 (2002) 324–331.
[24] Z. Chen, T. Zeng, B. Qian, J. Ding, Complete shaping of optical vector beams, Opt. Express 23 (2015) 17701–17710.
[25] P.L. Greene, D.G. Hall, Focal shift in vector beams, Opt. Express 4 (1999) 411–419.
[26] S. Yan, B. Yao, R. Rupp, Shifting the spherical focus of a 4Pi focusing system, Opt. Express 19 (2011) 673–678.
[27] Z. Li, S. Yan, B. Yao, M. Lei, B. Ma, P. Gao, D. Dan, R. Rupp, Theoretical prediction of three-dimensional shifting of a spherical focal spot in a 4Pi focusing system, J. Opt. 14 (2012) 055706.
[28] Y. Yang, M. Leng, Y. He, H. Liu, Q. Chang, C. Li, Focal shift in spatial-variant polarized vector Bessel-Gauss beams, J. Opt. 15 (2013) 014003.
[29] B. Richards, E. Wolf, Electromagnetic diffraction in optical systems II. Structure of the image field in an aplanatic system, Proc. R. Soc. London Ser. A 253 (1959) 358–379.
[30] Q. Zhan, Cylindrical vector beams: from mathematical concepts to applications, Adv. Opt. Photon. 1 (2009) 1–57.
[31] X. Wang, J. Ding, W. Ni, C. Guo, H. Wang, Generation of arbitrary vector beams with a spatial light modulator and a common path interferometric arrangement, Opt. Lett. 32 (2007) 3549–3551.
[32] H. Chen, J. Hao, B. Zhang, J. Xu, J. Ding, H. Wang, Generation of vector beam with space-variant distribution of both polarization and phase, Opt. Lett. 36 (2011) 3179–3181.
[33] Y. Pan, Y. Li, S. Li, Z. Ren, L. Kong, C. Tu, H. Wang, Elliptic-symmetry vector optical fields, Opt. Express 22 (2014) 19302–19313.
[34] S.W. Hell, J. Wichmann, Break the diffraction resolution limit by stimulated emission: stimulated emission-depletion fluorescence microscopy, Opt. Lett. 19 (1994) 780–782.
[35] L. Su, G. Lu, B. Kenens, S.A. Rocha, E. Fron, H. Yuan, C. Chen, P.V. Dorpe, M.B.J. Roeffaers, H. Mizuno, J. Hofkens, J.A. Hutchison, H. Ujii, Visualization of molecular fluorescence point spread functions via remote excitation switching fluorescence microscopy, Nat. Commun. 6 (2015) 6287.
[36] C. Min, Z. Shen, J. Shen, Y. Zhang, H. Fang, G. Yuan, L. Du, S. Zhu, T. Lei, X. Yuan, Focused plasmonic trapping of metallic particles, Nat. Commun. 4 (2013) 2891.
[37] Y. Zhang, J. Wang, J. Shen, Z. Man, W. Shi, C. Min, G. Yuan, S. Zhu, H.P. Urbach, X. Yuan, Plasmonic hybridization induced trapping and manipulation of a single Au nanowire on a metallic surface, Nano Lett. 14 (2014) 6430–6436.
[38] O. Masihzadeh, P. Schlup, R.A. Bartels, Enhanced spatial resolution in third-harmonic microscopy through polarization switching, Opt. Lett. 34 (2009) 1240–1242.
[39] F. Lu, W. Zheng, Z. Huang, Coherent anti-Stokes Raman scattering microscopy using tightly focused radially polarized light, Opt. Lett. 34 (2009) 1870–1872.
[40] Y. Iketaki, H. Kumagai, K. Jahn, N. Bokor, Creation of a three dimensional spherical fluorescence spot for super-resolution microscopy using a two-color annular hybrid wave plate, Opt. Lett. 40 (2015) 1057–1060.
[41] H. Kano, S. Mizuguchi, S. Kawata, Excitation of surface-plasmon polaritons by a focused laser beam, J. Opt. Soc. Am. B 15 (1998) 1381–1386.
[42] Q. Zhan, Evanescent Bessel beam generation via surface plasmon resonance excitation by a radially polarized beam, Opt. Lett. 31 (2006) 1726–1728.
[43] W. Chen, Q. Zhan, Realization of an evanescent Bessel beam via surface plasmon interference excited by a radially polarized beam, Opt. Lett. 34 (2009) 722–724.
[44] K.S. Youngworth, T.G. Brown, Focusing of high numerical aperture cylindrical vector beams, Opt. Express 7 (2000) 77–87.